

## Directions of Discontinuous Changes in Magnetization in Monocrystal Bars and Disks of Silicon-Iron

R. F. CLASH, JR. AND F. J. BECK, JR., *Sloane Physics Laboratory, Yale University*

(Received December 3, 1934)

### INTRODUCTION

BECK and McKeehan,<sup>1</sup> expecting to find a crystallographic dependence of the Barkhausen effect, looked for it in a stationary disk subjected to a rotating field of constant magnitude. They measured, with a two-element galvanometer (G. E. oscillograph) the amplified impulses in two search coils about the disk with their axes at right angles. The measurement of the rectangular components of a single discontinuity in magnetization, thus picked out, permits its relocation in the plane of the disk. They were unsuccessful in proving any important influence of crystal structure but McKeehan and Clash<sup>2</sup> in a preliminary report of further work done by the improved method described below, were able to show that the expected dependence existed. The principal improvement in technique consisted in the use of a cathode-ray oscillograph which provides a means whereby the two amplified component impulses could be impressed upon a single moving element, the electron beam, and thus reintegrate the parts into a vector representing the nearly discontinuous increment in magnetization,  $\Delta I$ . The excursions of the luminous spot on the fluorescent screen would then be nothing more than two dimensional reconstructions of the initial  $\Delta I$ 's. The modifications that were necessary in the apparatus warrant complete description at this time.

We now have data taken on a number of specimens which appear to justify the working hypothesis earlier presented.<sup>2</sup>

### APPARATUS

#### 1. Effect-producing mechanism

In Fig. 1 a side view of the revised mechanism is shown. The self-supporting field coils used by Beck and McKeehan have been replaced by a

machined brass casting,  $G$ , to which a removable two-section magnetizing coil,  $F$ ,  $F'$ , may be clamped. Each of these sections is wound with 317 turns of No. 16 B. and S. gauge (0.1291 cm) enameled copper wire with single covered cotton insulation. The coil pair in series aiding produces a field intensity of 34.7 oersteds ampere<sup>-1</sup> as found by calibration with a Hibbert standard. In addition to increasing the field range the new arrangement gave improved mechanical performance.

The mirror system shown at  $E$ ,  $E'$  provides a convenient reference frame for making observations. Thirty-six small aluminum-on-glass mirrors, mounted at 10° intervals on the periphery of a hard rubber disk, form successive reflecting surfaces for a convergent beam of light, refocused (after reflection) on the ceiling of the room. Successive coincidences of the moving images with a stationary image (from a fixed mirror  $E'$ ) provide a convenient method of counting the 10° intervals. One moving image is double, furnishing a conspicuous starting point for counting the intervals. A reflection is designated by an integer,  $N$ , ranging from 0 to 35 ( $N=0$  for the double moving image).

A new rectangular search coil system (see Fig. 2) has been constructed in which the two coils  $J$ ,  $J'$  have equal areas and numbers of turns. Also the specimen,  $K$ , may be placed at a position similarly related to both coils, so that the coils become equivalent. Each coil is wound with a total of 5000 turns of No. 40 B. and S. gauge (0.0080 cm) enameled copper wire (2500 turns per channel). The windings of the two channels,  $L$ ,  $L'$ , of a coil are connected in series aiding, and have a total resistance of about 2100 ohms. The angular position of the coil system is adjustable and easily determined from a calibrated circular scale on the mounting.

Special precautions were taken to insure uniform rotation of the effect-producing mechanism with a minimum of mechanical vibration. The driving torque was furnished by a single phase,

<sup>1</sup> F. J. Beck, Jr., and L. W. McKeehan, *Phys. Rev.* **41**, 385 (1932); **42**, 714-720 (1932).

<sup>2</sup> L. W. McKeehan and R. F. Clash, Jr., *Phys. Rev.* **45**, 839-840 (1934).

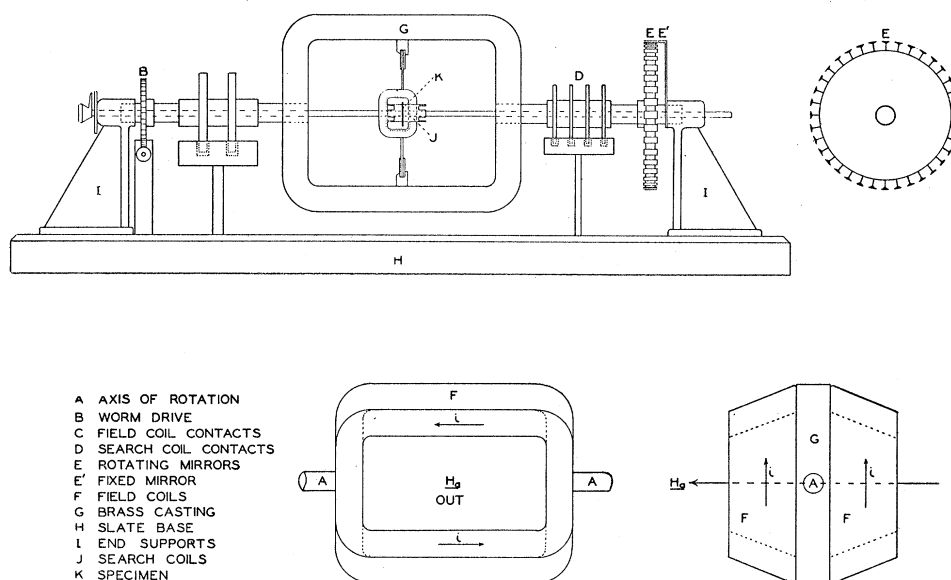


FIG. 1. Side view of the revised rotating mechanism, axial view of mirror system, and side and axial views of the new field coils clamped to the supporting brass casting.

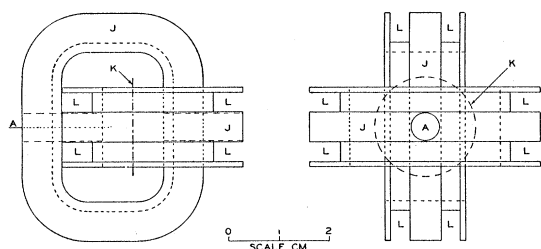


FIG. 2. Side and axial views of the new search coils. Note the equivalence of the two rectangular sections and their positions relative to the stationary specimen. Forms are of hard rubber. A, axis of rotation; J, search coil form; K, specimen; L, channel for windings.

60 cycle, 1/50 h.p., 1200 r.p.m., Westinghouse synchronous motor working through 5000 : 1 reduction gears. Motor and one reduction gear were mounted rigidly and "floated" on a hair-felt pad, this assembly being located about 180 cm from the mechanism proper. One section of the connecting drive shaft was a (0.95 cm) lead pipe. The magnetic field and search coil system were thus rotated about the stationary specimen once in 250 seconds.

## 2. The amplifiers

Two 4-stage resistance-capacity coupled audio-frequency amplifiers were constructed. The circuit constants are shown in Table I. One side of

TABLE I. Circuit constants of amplifier.

Stage	Tube	$E_b$	$E_g$	$R_p$	$R_g$	C
1	PJ-11	180v	-1.2v	0.1 Meg.	—	0.1 $\mu$ f
2	UX-240	270v	0	0.75 "	5 Meg.	0.1 $\mu$ f
3	UX-240	270v	0	0.75 "	5 "	0.1 $\mu$ f
4	UX-240	225v	-4.5v	0.25 "	5 "	0.1 $\mu$ f

each search coil was connected directly to the grid of its respective amplifier while the other was grounded, thus impressing the induced emf's directly on the input grids. The PJ-11 gave satisfactorily low noise output.<sup>3</sup> The grid bias of the output tube made it necessary to adjust the signal "sense" so as to produce positive grid swings from this bias value. This eliminated distortion, but confined observations to excursions occurring in one quadrant of the oscillograph screen. The total voltage amplification realized from this circuit was about 147,000.

## 3. The oscillograph

Some difficulty was experienced in finding a cathode-ray oscillograph with sufficient photographic intensity and deflector plate sensitivity. Finally a DuMont<sup>4</sup> Type 54 (5 inch screen, 2 sets

<sup>3</sup> G. F. Metcalf and T. M. Dickinson, *Physics* 3, 11 (1932).

<sup>4</sup> We very gratefully acknowledge the help and sugges-

of orthogonal deflector plates) tube was chosen. This was operated with an accelerating potential of 2000 volts, and a focusing potential of about 325 volts, giving a deflector plate sensitivity of approximately  $0.4 \text{ mm volt}^{-1}$ . Search coil leads, windings and oscillograph excursions were so related that permissible observations were confined to the third quadrant of the fluorescent screen. Experimental conditions were adjusted as necessary to meet this requirement.

#### 4. Operation

Data were taken with this revised apparatus by two procedures. The first involved photographing the excursions by means of a laboratory-made camera fitted with an adjustable aperture F1.9 lens and using standard 35 mm film (supersensitive gray-back panchromatic). Successive short exposures were taken at  $10^\circ$  intervals giving a complete set of data in 250 seconds. It was found that optimum photographic contrast was obtained for an exposure time equal to the  $(F \text{ setting})^2/120$  seconds. For longer exposures general illumination of the fluorescent screen produced excessive halation on the film. The most conspicuous excursions were then traced by a sharp pencil on thin translucent paper, and their angles relative to the oscillographic axes measured with a protractor.

The other procedure necessary in some cases, was to count individual excursions occurring within  $10^\circ$  intervals having lengths greater than an arbitrary minimum  $r$ . This was accomplished by successively placing opaque circular screens of proper radii over the center of the fluorescent screen. This required two workers, one for counting, the other for recording while the photographic experiments were easily conducted by a single operator.

It is of importance to remark that adequate shielding of the apparatus from mechanical, acoustical and electromagnetic disturbances was necessary. Each amplifier had two independent sets of batteries and separately shielded compartments for each stage. Further, the mechanism proper was enclosed in a copper box, and all exposed leads carefully shielded.

tions of Mr. Allen B. DuMont in finding a cathode-ray oscillograph meeting our requirements.

#### REFERENCE SYSTEM

In Fig. 3 we have drawn the search coil axes,  $S_x, S_y$ , in an arbitrary position with the field vector,  $\mathbf{H}_a$ , making an angle  $\gamma$  with the positive  $S_x$  direction. This angle may be adjusted at will, but remains constant during a run. Obviously the differential field vector  $d\mathbf{H}_a/dt$  is constant in magnitude and leads the field vector by  $90^\circ$  when the latter has a constant magnitude and rotates at a uniform rate. It will also be noted from the figure that our previously defined integer,  $N$ , has its zero value at the instant  $\mathbf{H}_a$  is parallel to the fiducial mark on the stationary specimen. Now since the oscillograph axes correspond to  $S_x$  and  $S_y$  we may at once find the angle  $\psi$  between the reference mark on the specimen and  $\Delta I$  if  $\theta$  is known ( $\theta$  is the angle between  $S_x$  and  $\Delta I$  found from the photograph). By inspection we see that

$$\psi = \theta - \gamma + 10N, \quad (1)$$

$$\phi = \psi - 10(N+9), \quad (2)$$

where  $\phi$  is the angle between  $d\mathbf{H}_a/dt$  and  $\Delta I$ .

The high impedance coupling of the ungrounded plate of a pair of the deflector plates to ground introduced a non-orthogonality of the oscillograph axes as photographed, and made it necessary to add a correction term to  $\theta$ , depending only upon its observed magnitude. This correction ranged from  $0^\circ$  to  $5^\circ$ .

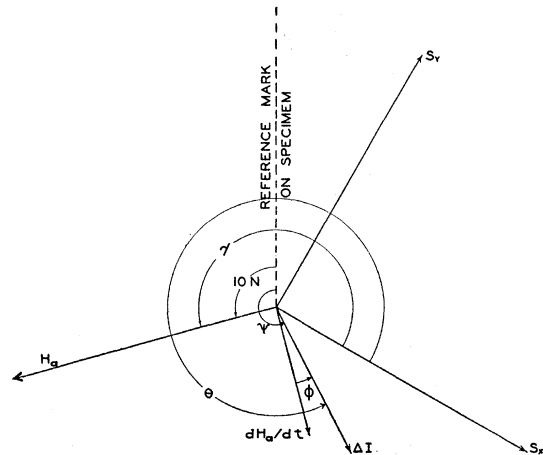


FIG. 3. Reference system. The reader must conceive of all vectors as rotating with respect to the dotted line which is fixed on the plane of the specimen. All of these vectors except  $\Delta I$  are fixed relative to one another.

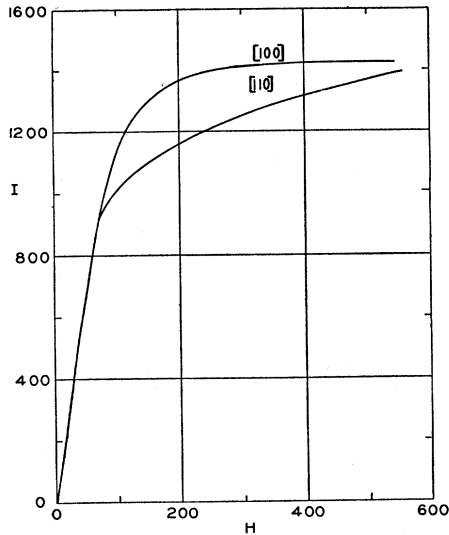


FIG. 4. Magnetization of silicon-iron single crystals along  $[100]$  and  $[110]$  directions as a function of the magnetizing force in oersteds.

### Specimens

All the disk and bar specimens, except the polycrystal disk of specially processed<sup>5</sup> electrical sheet steel were cut from material very kindly furnished us by Dr. W. E. Ruder of the General Electric Company's Research Laboratories. This stock was in strip form and had the following average composition.

C	Mn	P	S	Si
0.05	0.15	0.038	0.026	3.24

A small ellipsoid was ground from this material and analyzed magnetically by the modified Curie balance since described by McKeehan.<sup>6</sup> Fig. 4 shows the magnetization curve obtained for the two crystallographic directions,  $[100]$  and  $[110]$ . The characteristic magnetic anisotropy of single crystals of silicon-iron is revealed.

No. 1 (100) disk  
Diameter—1.33 cm  
Thickness—0.022 cm  
Demagnetizing factor—0.16

No. 2 (100) disk  
Diameter—1.51 cm  
Thickness—0.018 cm  
Demagnetizing factor—0.12

No. 3  $[100]$  disk  
Diameter—2.54 cm  
Thickness—0.0457 cm  
Demagnetizing factor—0.17.

The projected crystallographic directions for the disks (of the form  $\langle 100 \rangle$ ) are indicated in Figs. 5, 6 and 7.

Polycrystal disk (processed electrical sheet steel)

Diameter—1.51 cm

Thickness—0.0328 cm

(100) Bar— $1.90 \times 0.28 \times 0.05$  cm<sup>3</sup>

Axis of bar  $14.9^\circ$  from  $[100]$ , normal to plane of bar at  $75.1^\circ$  from  $[100]$ .

(110) Bar— $1.92 \times 0.28 \times 0.05$  cm<sup>3</sup>

Axis of bar  $21.3^\circ$  from  $[110]$ , normal to plane of bar at  $68.7^\circ$  from  $[110]$ .

Polycrystal bar— $1.92 \times 0.29 \times 0.05$  cm<sup>3</sup>. This specimen was cut from the same strip as were the two above, but consisted of a large number of small random grains.

### RESULTS

All three of the bar specimens gave a single sharply defined linear trace on the oscillograph screen. The trace lengths were also approximately equal for corresponding directions of  $H_a$ . Table II gives the angles between the bar length and the observed  $\Delta I$ 's for all three specimens at two values of  $H_a$ . It will be noted that all observed

TABLE II. Azimuth angles. Bar specimens.

Spec.	(100)		(110)		Polycrystal	
	$H_a$					
$N$	86.9	156.3	86.9	156.3	86.9	156.3
4						
5	181	181	175	175	179	180
6	178	178	177	176	177	178
7	177	177	179	178	177	180
8	178	178	176	176	178	180
9	177	177	179	177	177	176
10	179	177	176	176	179	178
11	178	179	176	174	179	178
12	179	179	176	176	179	178
13	181	180			176	177
14						
-----						
22						
23	0	0	358	354	0	0
24	358	359	355	355	359	0
25	359	358	356	356	0	0
26	356	358	355	355	359	359
27	358	357	358	359	0	359
28	1	358	359	358	359	0
29	0	0	357	357	358	359
30	358	359	357	356	0	358
31	1	359			357	1
32						

<sup>5</sup> N. P. Goss, United States Patent No. 1,965,559, also see reference Trans. A. S. M. 1934 (in press).

<sup>6</sup> L. W. McKeehan, Rev. Sci. Inst. 5, 265 (1934).

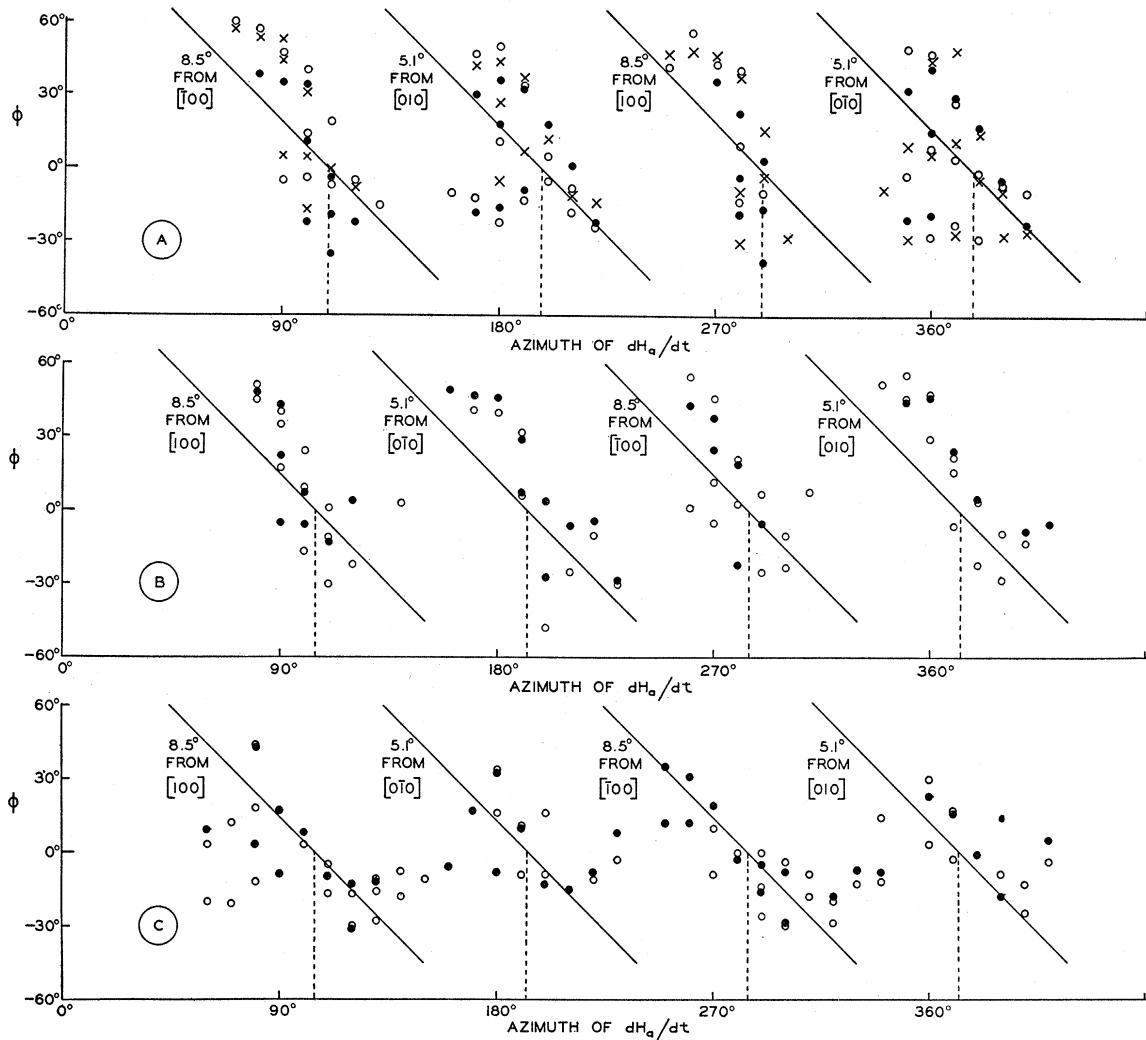


FIG. 5. Photographic results for No. 1 (100) silicon-iron disk. *A*, unannealed, three runs;  $\times$   $I=1363$ ,  $\circ$   $I=1360$ ,  $\bullet$   $I=1369$ ; *B*, annealed, two runs  $\circ$   $I=1358$ ,  $\bullet$   $I=1353$ . The sum of the ordinate and abscissa of an observed point represents the angle between  $\Delta I$  and the arbitrary zero line on the specimen. Points lying on the full diagonal lines represent  $\Delta I$ 's parallel to the projected crystal direction as indicated. The dotted lines represent the angles at which  $d\mathbf{H}_a/dt$  is parallel to the respective crystal directions as marked. The crystallographic dependence consists in the occurrence of frequent  $\Delta I$ 's when  $d\mathbf{H}_a/dt$  is in the near vicinity of a direction of easiest magnetization, and a crowding of points near the diagonal lines.

changes in magnetization are parallel to the long axes of the bars.

In passing it should be noted that one revolution of the mechanism carries the bar through an ordinary hysteresis cycle since only that component of  $\mathbf{H}_a$  which is parallel to the length of such a bar is effective in magnetizing it appreciably. As is to be expected the rotating linear pattern has two zeros and two maxima per cycle, these latter occurring when the steep parts

of the hysteresis curve are being traversed.

The bar data indicate at once that our first concept of these changes as due to reversals of single domains along axes of a single form, here  $\langle 100 \rangle$ , is incorrect and that more complicated processes occur. These data have a further significance in that they show the equivalence of the two search-coil-plus-amplifier systems. The same results were obtained by having the two systems "trade" components. This is an im-

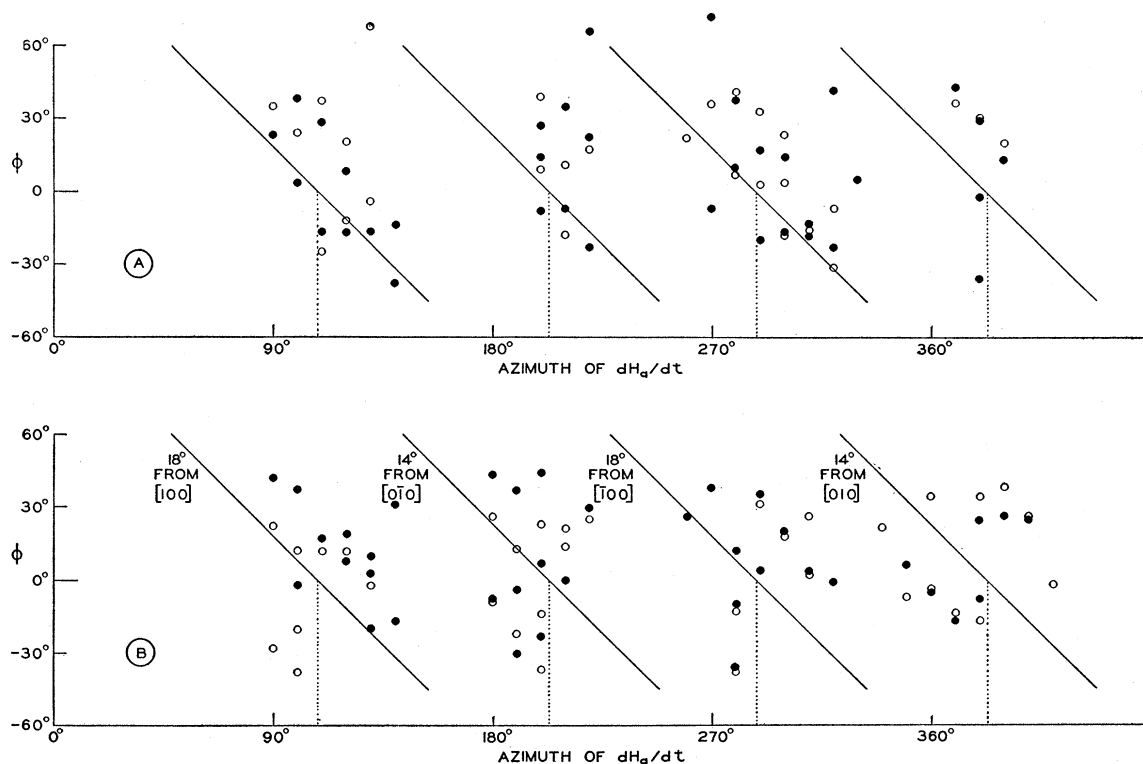


FIG. 6. Photographic results for No. 2 silicon-iron disk. *A*, annealed, two runs  $\circ I=1273$ ,  $\bullet I=1273$ ; *B*, annealed, two runs  $\circ I=1360$ ,  $\bullet I=1358$ . See caption of Fig. 5 for explanation.

portant verification since it directly tests the operation of the apparatus under simple conditions.

Fig. 5 and Fig. 6 show the data obtained from photographs for two (100) single crystal disks of silicon-iron. It is important to note that the crystallographic dependence here shows up so clearly because only excursions too short for resolution are present when  $d\mathbf{H}_a/dt$  is parallel to directions of the form  $\langle 110 \rangle$ . The "counting" method is necessary in cases where excursions long enough for photographic recording occur at all angles. Fig. 7 is an example. This specimen is the one used previously by Beck and McKeehan in which no apparent crystallographic dependence was found. The unweighted angles,  $\psi$ , then studied are now seen to be of secondary importance and our attention is directed to those azimuths of  $d\mathbf{H}_a/dt$  for which excursions of greater length are found. We naturally assume that these correspond to larger increments in magnetization.

The results of the counting method as applied to the "Goss" processed electrical sheet steel disk are shown in Fig. 8. The diagram, while not as striking, indicates the same type of fourfold symmetry exhibited by the single crystal of Fig. 7. The colloid concentration pattern,<sup>7</sup> Fig. 9<sup>8</sup> for a section of this material shows that there is a preference for surface magnetization along the rolling direction.

The disk specimens under the present experimental conditions exhibit several noteworthy characteristics. In the first place many excursions occur for which the corresponding  $\Delta\mathbf{I}$ 's have components antiparallel to the applied field,  $\mathbf{H}_a$ . This, of course, means that changes in magnetization take place for which the magnetic potential energy relative to the applied field shows an increase. This need not disturb us since

<sup>7</sup> L. W. McKeehan and W. C. Elmore, Phys. Rev. **46**, 226 (1934).

<sup>8</sup> Mr. W. C. Elmore of this laboratory kindly furnished us with this photograph.

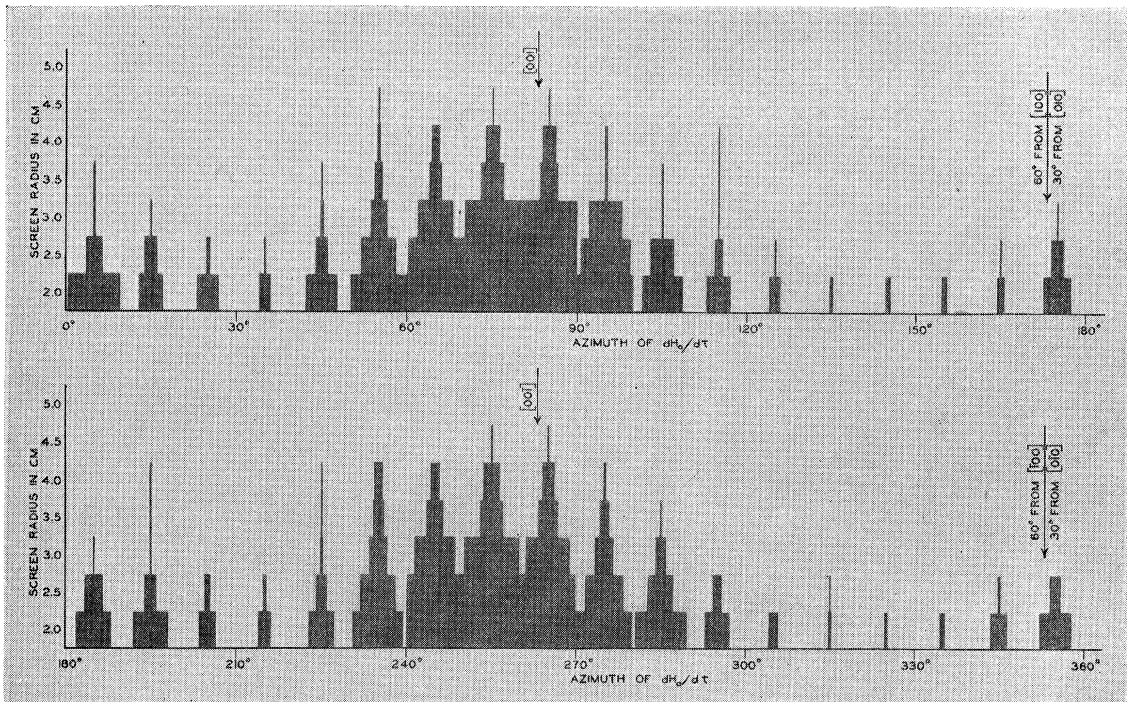


FIG. 7. Data for No. 3 silicon-iron single crystal disk.  $I=1190$ . The number of discontinuities having lengths greater than  $r$  are plotted as a function of the position of  $dH_a/dt$ . The width of a band represents the number counted in the interval required for  $dH_a/dt$  to rotate through  $10^\circ$ . A band "10" in width represents 30 discontinuities which is the value assigned to intervals having too many excursions for accurate count.

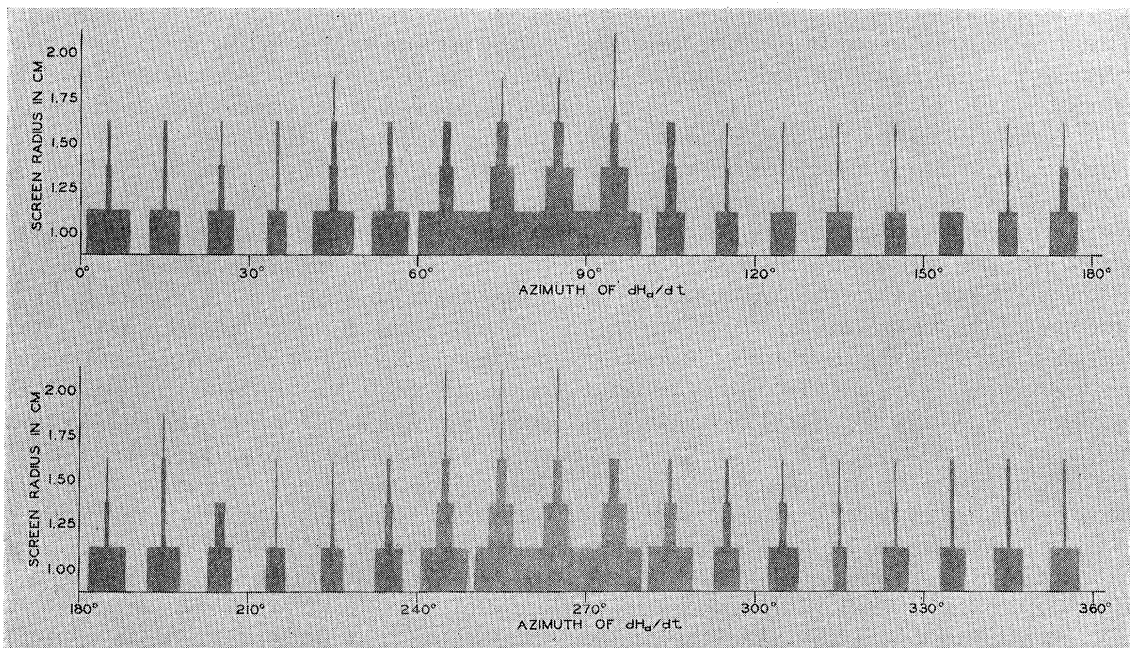


FIG. 8. Results for disk of silicon sheet steel furnished by N. P. Goss.  $H_a=139$ . See Fig. 7 for explanation. Here the width of a band represents 25 discontinuities. The zero azimuth is parallel to the direction of rolling,  $90^\circ$  and  $270^\circ$  representing the transverse direction.

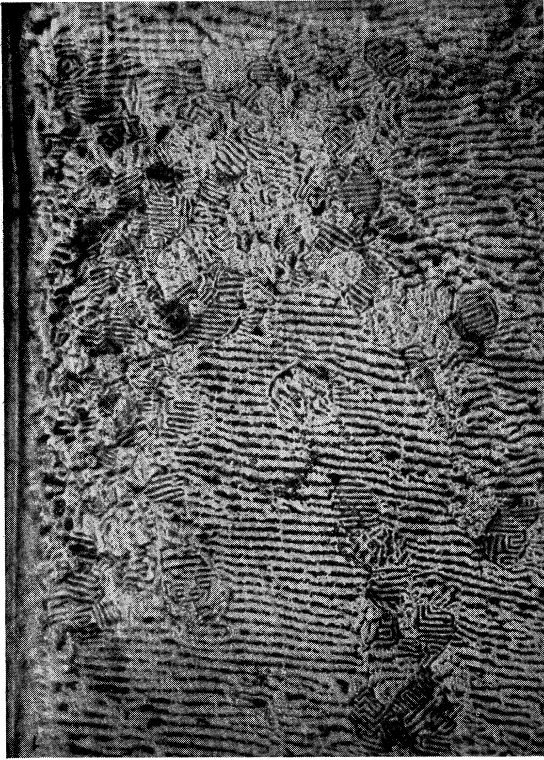


FIG. 9. Colloid concentration pattern for a section of the disk of silicon sheet steel furnished by N. P. Goss. The rolling direction is along the scratch on the left side of the pattern.

we expect large variations in the macroscopic field intensity from point to point inside the crystal at magnetizations below saturation. These local fields may be conceived of as causing the resulting  $\Delta I$ 's observed. Hence the anomaly is apparent rather than real.

A second peculiarity noted only in the case of the disk specimens is the occurrence of many curved and zigzag traces. These indicate a change in direction of  $\Delta I$  during the time of tracing. We appear to have passed from the simple one-dimensional bar specimen to the case where two degrees of magnetic freedom exist. Certainly such behavior as observed is unlikely if a single domain accounts for each observed effect by simple reversal of moment. On this simple picture the (110) bar should have yielded a dual set of linear traces. As it did not, we now have two strong experimental points in favor of a "complicated" process.

The final important characteristic of disk specimens is obtained from Figs. 7 and 8 and from visual observation of the oscillograph excursions; namely, the longer excursions appear more frequently when  $dH_a/dt$  is in the near vicinity of a direction of easiest magnetization. The evidence strongly supports a crystallographic dependence of the Barkhausen effect.

As pointed out earlier<sup>2</sup> we look to the work of Sixtus and Tonks<sup>9</sup> for an explanation of the effects observed here. Under this view an observable and nearly discontinuous change in magnetization is conceived of as originating at a favorable nucleus, rapidly traveling to an end point and exhibiting on a much finer scale the same properties as those ascribed to the abnormally large discontinuities that have been produced in strained ferromagnetics. Such a change in magnetization would involve numerous ferromagnetic domains which together give complicated  $\Delta I$ 's under the conditions of macroscopic fields. This fits the marked angular spreading found which is in accord with Brion's work.<sup>10</sup> It furthermore anticipates a crystallographic dependence since larger regions would be involved if the process progressed mostly by reversals. This is obvious since a reversed domain subjects its end-on neighbors to the maximum favorable field variation. A train of reversals would then proceed farthest and produce the largest  $\Delta I$  if occurring when  $dH_a/dt$  coincided nearly with a direction for easy reversal. In the partly magnetized specimen below the knee of the curve a traveling reversal still finds the individual domains oriented along the few crystallographically stable directions, but of course, with a different distribution among these permitted directions than is appropriate to the demagnetized state.

We wish to express our sincere thanks to Professor N. I. Adams, Jr. for his help in connection with the design of the amplifiers and to Professor L. W. McKeehan for his continued interest and encouragement throughout the course of the investigation.

<sup>9</sup> K. J. Sixtus and L. Tonks, *Phys. Rev.* **35**, 1441 (1930); **37**, 930 (1931); **39**, 357 (1932); **42**, 419 (1932); L. Tonks and K. J. Sixtus, *ibid.* **41**, 539 (1932); **43**, 70-80; **43**, 931 (1933).

<sup>10</sup> H. Brion, *Ann. d. Physik* **15**, 167 (1932).





FIG. 9. Colloid concentration pattern for a section of the disk of silicon sheet steel furnished by N. P. Goss. The rolling direction is along the scratch on the left side of the pattern.